Divergent Nanostructures from Identical Ingredients: Unique Amphiphilic Micelle Template for Polyaniline Nanofibers, Tubes, Rods, and Spheres

P. Anilkumar[†] and M. Jayakannan*[,‡]

Chemical Sciences & Technology Division, National Institute for Interdisciplinary Science and Technology, Thiruvananthapuram 695019, Kerala, India, and Department of Chemistry, Indian Institute of Science Education and Research (IISER), NCL Innovation Park, Dr. Homi Bhabha Road, Pune 411008, India

Received May 15, 2008; Revised Manuscript Received August 7, 2008

ABSTRACT: Here, we report a unique soft templating approach based on an in-built amphiphilic azobenzenesulfonic acid for tuning various types of polyaniline nanomaterials such as fibers, rods, spheres, and tubes. The dopant molecule is freely soluble in water, and DLS measurements of the resultant solution revealed that it forms spherical micelles of diameter ~4.29 nm. The addition of aniline induces self-organization in the dopant micelles which produce micrometer-sized cylindrical aggregates or layerlike assemblies depending upon the aniline/dopant composition in the feed. In the emulsion route, the oxidation of these cylindrical or layerlike micelle aggregates produce nanofibers and nanotubes, respectively. The dilution of thick emulsion microaggregates led to the formation of uniformly distributed small 175 nm aggregated micelles, which template for the nanorods (dilution route). Alternatively, the dopant micelles form spherical shape aggregates with oxidizing agent ammonium persulfate (APS) in water. Aniline molecules diffuse through the organic/aqueous interface and get absorbed at these spherical aggregates, and subsequent chemical oxidation produces exclusively polyaniline nanospheres (interfacial route). The mechanism of the polyaniline nanomaterials formation was investigated by dynamic light scattering (DLS) and high-resolution transmission electron microscopy (TEM). DLS studies of the polymerization mixtures in water evident for the formation of micrometer range aggregates. TEM analysis confirmed the shape of the template as cylindrical, cylindrical + spherical, and spherical geometry for the complexes of dopant with aniline and APS in the emulsion, dilution, and interfacial routes, respectively. The amphiphilic nature of the dopant solubilizes the nanomaterials in water and organic solvents, and the optical properties of nanomaterials were studied in various solvents by UV−vis spectroscopy. The wide-angle X-ray diffraction studies confirmed the appearance of a new peak at lower angle (d = 13.6 Å) corresponding to the highly crystalline and ordered polyaniline nanomaterials. The solid-state properties of the nanomaterials were found to be highly dependent on the size and shape of polymerization templates employed for the synthesis.

Introduction

Conducting polyaniline nanomaterials have been widely studied in recent years due to its tunable conductivity from nonconducting to metallic form,[1] good environmental stability,[2] and potential for applications in electronic devices[3−5] and chemical sensors,[6−8] etc. One-dimensional nanostructures of conducting polyaniline have been prepared both chemical[9] and electrochemical[10] polymerization of the aniline with the aid of external hard[11] or soft templates.[12] Though the hard template method has advantage that the length and diameter of the nanomaterials can be controlled by membrane pores,[11] it became less attractive due to tedious purification and poor stability of synthesized nanomaterials after the removal of templates,[13] etc. Soft template approaches like micelles[14−17] and gels[18,19] were developed to overcome the above limitations and employed in polymerization routes like emulsion,[20] interfacial,[21,22] rapid mixing,[23] seeding,[24] and dilute,[25−27] etc. Most often, the synthesis of polyaniline nanofibers was found highly susceptible to the reaction conditions such as method of oxidant addition,[23] reaction temperature,[28] and extent of stirring,[29] etc., and good homogeneous nanomaterials were produced only for selected experimental conditions. The reason for the inhomogeneity in the nanomaterials was understood as the poor stabilities of micelles or templates of the reacting constituents under the polymerization conditions.[30] Both interfacial and dilute polymerization are important nontemplate routes to synthesize high-quality polyaniline nanofibers. The advantage of these polymerization approaches is that the aniline monomer concentration is very low, and hence the secondary growths of nanofibers are prevented.[22,31] In conventional polymerization (like emulsion route), aniline concentration is expected to be relatively high and the competition between directional fiber growth process and formation of additional nucleation centers producing irregular shapes. In dilute solution (also interfacial route) the number of nucleation sites formed on the surface of the nanofibers is reduced, thus allowing polyaniline to grow only in one-dimensional morphology.[31,32] However, low yield, inability to large-scale synthesis, and structural restriction to a few acid dopants are unsolved problems associated with these superior processes. To the best of our knowledge, no detailed study has been done to analyze the influence of the structural changes of templates in emulsion, dilute, or interfacial route on polyaniline nanomaterials morphology. Further, a wider discrepancy was also noticed in the polyaniline nanomaterials synthesis over the selection of dopant molecules and polymerization routes: for instance, an emulsion-friendly dopant failed as a good candidate for interfacial or dilution routes and vice versa.[22] It restricts the deep understanding of the mechanistic aspects of polymerization processes and their dependency on the formation of nanomaterials.

Recently, we have developed a renewable resource strategy for polyaniline nanomaterials based on a raw material cardanol,

* Corresponding author: e-mail jayakannan@iiserpune.ac.in, Fax 0091-20-25898022.
[†] National Institute for Interdisciplinary Science and Technology.
[‡] Indian Institute of Science Education and Research.

10.1021/ma801090f CCC: $40.75
Published on Web 09/27/2008

Table 1. Dopant/Aniline Ratio, S/N Ratio, Yield, Conductivity, Dimensions, and WXRD Data of Polyaniline Nanomaterials

sample	conc of dopant (M^{-1})	conc of aniline (M^{-1})	yield[a] (%)	S/N[b] (%)	fiber diameter[c] (nm)	conductivity[d] σ (S cm^{-1})	[$I(2\theta)6.4$)/$I(2\theta)25.9$)][e]
E-70	5.1×10^{-3}	0.36	90	30.1	160–205	1×10^{-2}	0.25
E-100	3.2×10^{-3}	0.36	71	30.1	150–200	7.5×10^{-3}	0.31
E-150	2.4×10^{-3}	0.36	76	29.8	185–260	1.1×10^{-2}	0.29
E-300	1.2×10^{-3}	0.36	75	29.9	180–250	9.5×10^{-3}	0.37
E-450	8.2×10^{-4}	0.36	81	29.7	175–265	3×10^{-3}	0.49
E-600	5.9×10^{-4}	0.36	60	28.8	175–240	7×10^{-3}	0.19
E-900	4.1×10^{-4}	0.36	60	27.9	190–270	2.4×10^{-2}	0.18
D-100a	2.4×10^{-3}	0.24	76	29.5	125–210	7.8×10^{-3}	0.44
D-100b	1.8×10^{-3}	0.18	59	28.6	140–220	1.5×10^{-2}	0.68
D-100c	1.2×10^{-3}	0.12	68	29.1	130–225	4.6×10^{-3}	0.69
D-100d	9×10^{-4}	0.09	58	27.5	0.7–1.3 μm	7.3×10^{-3}	0.82
D-100e	7.2×10^{-4}	0.07	63	27.1	0.6–1.4 μm	2.4×10^{-3}	0.82
I-100	3.6×10^{-3}	0.36	34	33.3	Sp, 400nm–2.1 μm	2.6×10^{-2}	2.1

[a] Calculated for isolated product. [b] Calculated from elemental analysis data. [c] The values are determined from the SEM images. The symbol Sp indicates sphere. [d] Values are obtained using four probe conductivity unit at 30 °C. [e] From wide-angle X-ray diffraction measurements at 30 °C. Detailed WXRD plots are available in the Supporting Information.

which is an industrial waste and pollutant from cashew nut industry.[33−36] A new amphiphilic molecule, 4-[4-hydroxy-2((*Z*)-pentadec-8-enyl)phenylazo]benzenesulfonic acid, was developed from cardanol and employed as a dopant to produce polyaniline nanomaterials. Here, we report a unique micellar soft template approach based on an in-built amphiphilic azobenzenesulfonic acid for tuning various types of polyaniline nanomaterials such as fibers, rods, spheres, and tubes through selective templating process in water. The current approach is unique and novel in the sense that all the starting materials are same (amphiphilic dopant, aniline, ammonium persulfate (APS), and water), but various nanomaterials were produced in a controlled way depending on how these constituents are self-organized and polymerized in water under normal conditions. During the chemical oxidative polymerization of aniline via the self-assembly process, amphiphilic dopant molecules form thermodynamically stable aggregates of inherent nanoscale dimensions in solution, which act as template for the overall morphology of the resulting polyaniline. Templates formed by the dopant−aniline complex in emulsion, dilute, and interfacial polymerization are characterized by DLS (in solution) and TEM (in solid state). In the emulsion route the dopants form either cylindrical micelles or bilayers with aniline monomer, and their oxidation yields nanofibers and nanotubes, respectively. Upon diluting the emulsion, it transformed into micelle aggregates of 175 nm size, which are seeds for nanorods. In the interfacial route the spherical aggregate formed by the dopant−APS complex acts as a template for nanospheres. The nanomaterials were characterized by SEM, TEM, absorption spectroscopy, and X-ray diffraction to understand the morphology, electronic, and solid-state ordering. The amphiphilic nature of dopant enhances the solubility of the nanomaterials, and they can be easily dispersed in various solvents like water, alcohol, chloroform, *o*-chlorobenzene, *m*-cresol, and *p*-xylene, etc. This is the first time a unique amphiphilic sulfonic acid was developed to form a variety of templates with aniline and APS to produce a wide range of nanomaterials of fibers, rods, tubes, and spheres.

Experimental Procedures

Materials. Aniline, ammonium persulfate (APS), sulfanilic acid, hydrochloric acid, and sodium hydroxide were purchased locally and purified. Cardanol was purified by double vacuum distillation at 3−4 mmHg, and the fraction distilled at 220−235 °C was collected. Dopant molecule 4-[4-hydroxy-2-((*Z*)-pentadec-8-enyl)phenylazo]benzenesulfonic acid was synthesized as reported earlier.[33]

General Procedures. For SEM measurements, polymer samples were subjected to a thin gold coating using a JEOL JFC-1200 fine coater. The probing side was inserted into a JEOL JSM- 5600 LV scanning electron microscope for taking photographs. Transmission electron microscope images were recorded using a FEI Tecnai 30G^2 S Twin HRTEM instrument at 100 kV. For TEM measurements, the water suspensions of nanomaterials were prepared under ultrasonic stirring and deposited on a Formvar-coated copper grid. Wide-angle X-ray diffractions of the finely powdered polymer samples were recorded by a Philips analytical diffractometer using Cu Kα emission. For dynamic light scattering (DLS) measurements, we used a Nano ZS Malvern instrument employing a 4 mW He−Ne laser ($\lambda = 632.8$ nm) equipped with a thermostated sample chamber. For all the DLS measurements HPLC quality (Merck, India) double distilled water is used. All the dopant solutions are centrifuged (2000 rpm, 5 min) prior to DLS measurements in order to remove any suspended particles, whereas the emulsions and dopant + APS complexes are not centrifuged since centrifugation may destabilize the emulsion. Infrared spectra of the polymers were recorded using a Perkin-Elmer, spectrum one FTIR spectrophotometer in the range of 4000−400 cm^{-1}. For conductivity measurements, the polymer samples were pressed into a 10 mm diameter disk and analyzed using a Keithley four-probe conductivity instrument by applying a constant current. The resistivity of the samples was measured at five different positions, and at least two pellets were measured for each sample: an average of 10 readings was used for conductivity calculations. The thermal stability of the polymers was determined using a TGA-50 Shimadzu thermogravimetric analyzer at a heating rate of 10 °C/min in nitrogen. UV−vis spectra of the PANI in water were recorded using Perkin-Elmer Lambda-35 UV−vis spectrophotometer. Specific conductance measurements are carried out using an Elico CM 185 model conductivity bridge. For all conductivity measurements deionized water was used.

Emulsion Route for Polyaniline Nanomaterials. A typical procedure for the synthesis of polyaniline nanomaterials is described in detail for **E-100**, and other samples were prepared following the same procedure. The dopant (0.053 g, 0.11 mmol) was dissolved in doubly distilled water (20 mL) and stirred under ultrasonic for 1 h at 30 °C. Distilled aniline (1 mL, 1.02 g, 11 mmol, [aniline]/[dopant] = 100) was added to the dopant solution and stirred under ultrasonic for an additional 1 h at 30 °C. At the end of the stirring, the formation of pale yellow emulsion was noticed. Ammonium persulfate (1.1 M solution) was added at 5 °C and stirred under ultrasonic for 1 h at 5 °C. The resultant green color content was allowed to stand at 5 °C for 15 h without being disturbed. The solid mass was filtered and washed with distilled water, methanol, and diethyl ether several times until the filtrate became colorless. The solid product was dried in a vacuum oven at 60 °C for 48 h (0.01 mmHg). Yield = 0.80 g (76%). FT-IR (in cm^{-1}): 3010.8, 1579.7, 1500.6, 1305.8, 1224.8, 1159.2, 1031.9, 825, 705.9, and 628.7.

The polyaniline samples **E-70** to **E-900** were prepared by varying [aniline]/[dopant] as 70, 100, 150, 300, 450, 600, and 900 by following the above procedure. The aniline/dopant ratios and yields of the nanofibers are given in Table 1.

Dilute Emulsion Route to Polyaniline Nanomaterials. A typical procedure for the synthesis of polyaniline nanomaterials is

described in detail for **D-100a**, and other samples were prepared following the same procedure. The dopant (0.053 g, 0.11 mmol) was dissolved in doubly distilled water (20 mL) and stirred under ultrasonic for 1 h at 30 °C. Distilled aniline (1 mL, 1.02 g, 11 mmol, dopant/aniline = 1:100) was added to the dopant solution and stirred under ultrasonic for an additional 1 h at 30 °C. The resulting emulsion was diluted by adding 15 mL of water. To this, ammonium persulfate (10 mL, 1.1 M solution) was added at 30 °C. The resultant green color content was allowed to stand at 30 °C for 15 h. The solid was filtered and washed with distilled water, methanol, and diethyl ether several times until the filtrate become colorless. The solid product was dried in a vacuum oven at 60 °C for 48 h (0.01 mmHg). In a similar way, the total volume of the reaction feed is varied by adding 30, 60, 90, and 120 mL of water by keeping the [aniline]/[dopant] as 100 to synthesize samples **D-100b**, **D-100c**, **D-100d**, and **D- 100e**, respectively. FT-IR (KBr, in cm^{-1}): 3013.6, 1561.2, 1486.3, 1304.1, 1251.8, 1153.4, 1103.3, 1029.9, 812.7, 705.4, and 616.4.

Interfacial Route for Polyaniline Nanomaterials. The dopant (0.053 g, 0.11 mmol) and ammonium persulfate (2.5 g, 11 mmol) were dissolved in doubly distilled water (30 mL) in a 50 mL glass vial. In a separate glass vial distilled aniline (1 mL, 1.02 g, 11 mmol, aniline/dopant = 100) was dissolved in dichloromethane. To the dichloromethane solution, dopant plus oxidant in water was carefully added without disturbing the interface. The interfacial polymerization was allowed to stand at 30 °C for 15 h without disturbing. Then the polyaniline solid mass was formed in the aqueous phase which was centrifuged and washed with distilled water and methanol several times until the filtrate become colorless. The solid product was dried in a vacuum oven at 60 °C for 48 h (0.01 mmHg). Yield = 0.36 g (35%). FT-IR (in cm^{-1}): 3015.8, 1563.5, 1484.3, 1301.2, 1248.8, 1151.4, 1106.3, 1027.9, 812.7, 707.4, and 618.4.

Results and Discussion

The amphiphilic azobenzene dopant molecule 4-[4-hydroxy-2-((*Z*)-pentadec-8-enyl)phenylazo]benzenesulfonic acid (see Figure 1) was synthesized from the renewable resource cardanol, which is an industrial waste from cashew nut processing industry. The cardanol was reacted with diazonium salt of sulfanilic acid in the presence of base to obtain the new dopant.[33,35] The molecule was purified by column chromatography, and the structure was confirmed by NMR, FT-IR, and mass spectroscopic techniques (see Supporting Information). The dopant has a unique built-in amphiphilic molecular design consisting of hydrophilic azobenzenesulfonic acid as polar head and long alkyl part as hydrophobic tail. Owing to the amphiphilic surfactant nature, the dopant molecule is soluble in water and forms a micellar soap-like solution[34] (see Figure 1). The addition of aniline into dopant micelles in water under ultrasonic stirring produced a thick yellowish milky emulsion. In order to tune the morphology of nanomaterials as well as to understand the mechanism of formation of nanomaterials, we have employed three synthetic approaches: (i) emulsions with varied ratio of aniline/dopant in the feed [from [aniline]/[dopant] = 1 to 900], (ii) kept the dopant/aniline ratio constant ([aniline]/[dopant] = 100) and diluted the resulting emulsion by adding water, and (iii) the polymerization is carried out in an aqueous/organic biphasic interfacial system. In approach 1, the concentration of aniline was fixed as 0.36 M whereas the dopant concentration was gradually decreased (3.6×10^{-1}–2.3×10^{-4} M) to produce a different aniline/dopant ratio. In approach 2, the dilution by the addition of water results in the decrease in both aniline and dopant concentration but without affecting the aniline/dopant molar ratio. The entire scenario of the synthesis of polyaniline nanomaterials using dopant is given in Figure 1. In general, most of the dopants so far reported in polyaniline synthesis (like CSA, ABSA, PTSA, salicylic acid, etc.) are less stable under experimental conditions, and stable emulsions were

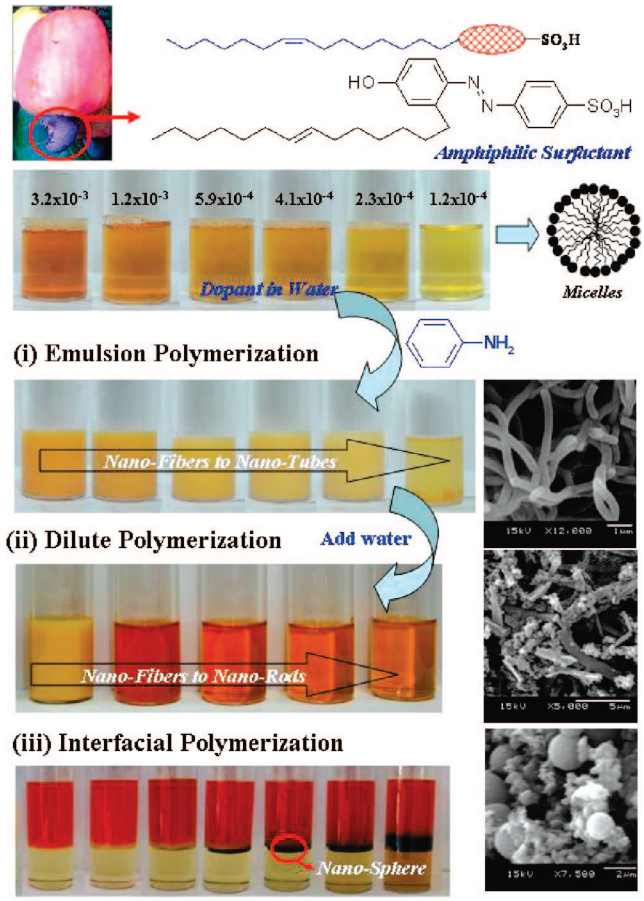

Figure 1. Synthesis of polyaniline nanomaterials using an azobenzene amphiphilic sulfonic acid by emulsion, dilute emulsion, and interfacial polymerization routes.

produced only for selected compositions. In Figure 1, the top photograph corresponds to the dopant in water and the visibility of the dopant changes in the range of 2×10^4 M, which corresponds to surfactant-like behavior. Interestingly, the amphiphilic dopant forms stable emulsion for a wide range of dopant/aniline ratios and are very stable for more than 1 month under normal ambient conditions. This gives the opportunity to trace both the effect of composition and concentration of the reactant constituents on the formation of nanomaterials. As the concentration of dopant is decreased lower than 2×10^{-4} M (for aniline/dopant >1200), the aniline + dopant complex is found to undergo phase separation (oil separated, see Figure 1). On the other hand, dilution by adding water into the preformed thick emulsion transformed into a clear solution without phase separation (see Figure 1). Unlike the emulsion route, in the dilution route the concentration of the aniline also decreases along with dopant, which accounts for the homogeneous solution. It suggests that the amphiphilic dopant is very versatile in nature, and a wide range of compositions of the reactants as well as their concentration can be fine-tuned for nanomaterials synthesis.

The emulsion and dilution polyemrization mixtures were oxidized by 1.1 M APS solution to obtain green polyaniline nanomaterials. Typically, the polymerization mixtures were oxidized by APS in water under ultrasonic stirring, and the resultant nanomaterials were purified by repeated washing with water and methanol until the filtrate become colorless. Polyaniline nanomaterials were produced in 60−80% yield. The samples prepared by emulsion route was denoted as **E-*X***, where ***X*** = aniline/dopant ratio in the feed. The samples prepared by the dilution method were denoted as **D-100*x***, where **x** = **a**, **b**, **c**, **d**,

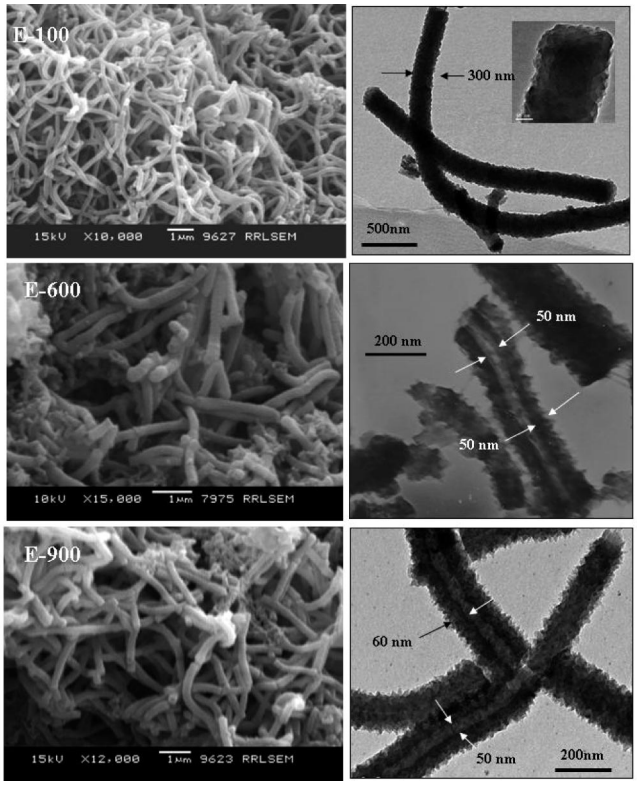

Figure 2. SEM and TEM images of polyaniline nanomaterials synthesized by emulsion polymerization.

and **e** (see Table 1). The concentrations of the aniline and dopant are given in table, and the exact amount of water added for dilution is given as Supporting Information. Interfacial polymerization is performed in an aqueous/organic two-phase system with aniline dissolved in dichloromethane, and ammonium peroxydisulfate + dopant were dissolved in an aqueous phase. Ammonium persulfate and dopant 1 were dissolved in water and immediately transferred to a vial containing aniline in dichloromethane. The ratio of the [aniline]/[dopant] was maintained as 100 (sample named as **I-100**) based on our previous experience in a similar system.[36] It is observed (within 2 min) that, upon adding APS solution, the aqueous dopant layer slowly transformed from clear yellow to turbid (see vials in Figure 1). After an induction period of 10 min, the polymerization started, and a green layer of polyaniline emeraldine appears at the interface. As the reaction proceeds, the green layer became thick. After 15 h, the entire aqueous layer turned to a dark solid. The aqueous layer was separated carefully, centrifuged, and washed well with water and methanol to remove all oligomers, excess dopant, and inorganic impurities. The polyaniline structure and doping of emeraldine salt by the sulfonic acid was confirmed by FT-IR analysis (see Supporting Information), and the degree of doping (S/N ratio) was determined from elemental analysis (see Table 1). Four probe measurements confirmed the bulk conductivity of the nanomaterials in the range of $\sim 10^{-3}-10^{-2}$ S/cm^{-1}, which are matching with that of the earlier reports.[14,30] The thermal stability of the nanomaterials was analyzed by TGA, and all the nanomaterials were found stable more than 300 °C (see Supporting Information).

The morphologies of the nanomaterials were characterized by a scanning electron microscope (SEM) and a transmission electron microscope (TEM), and the average length and diameters of the nanomaterials are determined from SEM images and summarized in Table 1. Typical SEM images of polyaniline synthesized by the emulsion route are given in Figure 2. The samples synthesized by the oxidation of thick emulsion (**E-100**) yields a mat of highly uniform nanofibers of diameter 180 nm and are very long up to 7 μm. Similarly, the SEM images of **E-600** and **E-900** also appear as nanofibers. Since the SEM technique is inadequate to see the internal features of nanofibers, the samples were subjected to TEM analysis. The TEM image of the sample **E-100** is matching with that of its SEM image and confirmed the presence of long nanofibers. The edge expanded inset of the fiber is also clearly support the solid nature of the nanofibers. Interestingly, the TEM image of **E-600** consists of a mixture of nanofibers plus nanotubes, and **E-900** is mostly in the form of nanotubes. It suggests that at lower dopant concentration (aniline/dopant $\geq$600) in the emulsion polymerization route the nanomaterials are transformed from nanofibers to nanotubes. The wall thickness of the nanotubes were found $\sim$50 nm with a pore diameter $\sim$50$-$70 nm. Most of the nanotubes are single walled, almost straight, and the length is as long as 1$-$2 μm. It is also interesting to note that the nanotubes also formed Y-junctions (see Supporting Information) as in the case of carbon nanotubes. One of the major concerns in the area of nanomaterials research is the lack of reproducibility and also the extent the approach to large-scale synthesis.[28] Most often polyaniline nanomaterials were reported in very low yield and mostly restricted to few milligram scales. Recently, Jing et al. reported that the polyaniline synthesis was also susceptible to experimental conditions like magnetic and ultrasonic stirring, and good fibers were produced only in selective conditions.[29] These issues are always a major concern for reproducible research in conducting polyaniline nanomaterials. In order to check the reproducibility of nanomaterials in our system, we have carried out control synthesis by varying experimental conditions like temperature (5, 30, and 50 °C) and ultrasonic irradiation, stirring using magnetic and without stirring, etc. Besides we have extended this approach to bulk scale synthesis of nanomaterials up to from 1 to 10 g scale and also various dopant/aniline ratios in the feed. The SEM images of the resultant samples and detailed procedures are shown in the Supporting Information. The nanofiber morphology of these controlled experiment samples was perfect under all conditions. It suggests that the amphiphilic azobenzene dopant employed here is very unique, and the properties of nanomaterials are solely dependent on dopant used rather than external stimuli like sonication and reaction temperature, etc. On the basis of the learning from these control experiments, in the current research, we have carried out all the experiments minimum at 1 g scale for reproducible research.

The SEM images of dilute polymerization route samples are given in Figure 3. The samples **D-100a** to **D-100c** consists of nanofibers of 140 nm thickness, which are thin compared to that of emulsion fibers (**E-100**). Largely diluted sample, **D-100d** mainly comprises of nanorods plus spheres instead of nanofibers. As the polymerization medium becomes very dilute (as in the case of **D-100e**), the sample comprises of only nanorods[37] of diameter ranging from 175 to 800 nm. The TEM images of **D-100d** (see Figure 3) revealed that the nanorods are formed by the aggregation of nanospheres. The contrast difference of the interior part and exterior part clearly suggests the noncylindrical shape of the nanorods, and the whiskerlike growth seen in rod surface indicates the adsorption of nanospheres. It is also interesting to see from the TEM images of **D-100e** that the rod composed of nanofibers of diameter $\sim$75 nm. On the basis of the TEM (also SEM) images, we believe that during the initial stages of polyaniline formation in very dilute polymerization both nanospheres and nanofibers are formed. During the course of reaction the spheres are adsorbed on nanofiber surface which leads to nanorod formation. The above assumption is supported by the fact that the SEM and TEM images of rod clearly indicate the noncylindrical shape mostly due to the surface adsorption

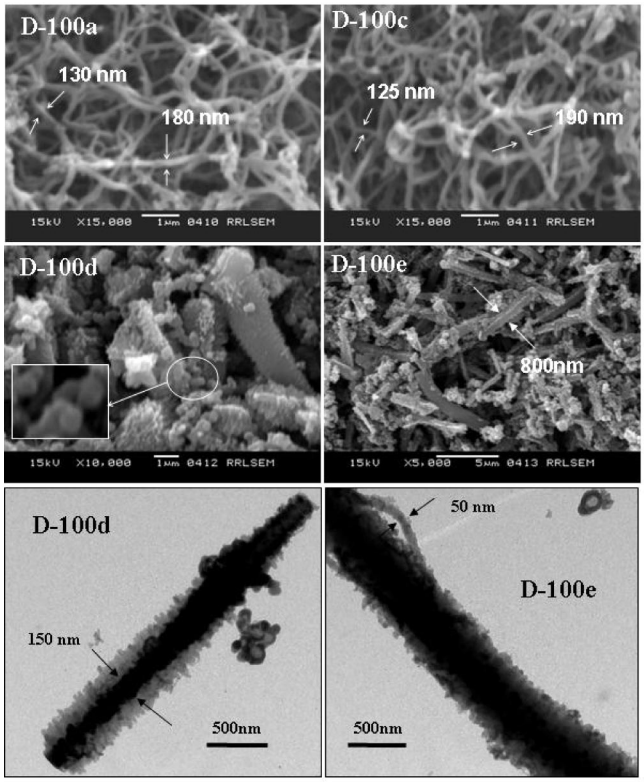

Figure 3. SEM and TEM images of polyaniline nanomaterials synthesized by dilute polymerization.

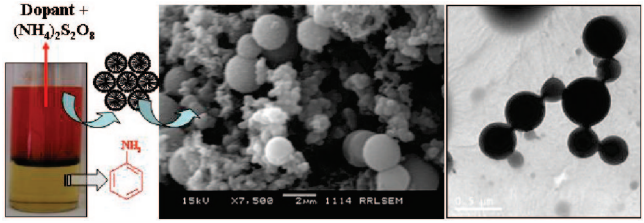

Figure 4. Synthesis and morphology of polyaniline nanospheres by interfacial polymerization.

of nanospheres over the initially formed nanofibers fragments. Nevertheless, from the morphological analysis, it is clearly evident that (i) the decrease in the dopant amount in emulsion route (decrease in the dopant/aniline ratio), the nanomaterials are transformed from nanofibers to nanotubes, and (ii) the decrease in the concentration of both aniline and dopant (for fixed aniline/dopant ratio = 100) results in the transformation of thin fibers to nanorods. SEM and TEM images of interfacial route sample (**I-100**) confirmed the presence of only nanospheres (see Figure 4). It suggests that the amphiphilic dopant follows a different pathway in the interfacial route to produce nanospheres compared to that of emulsion and dilution route. It is very important to note that in all the cases the starting materials are same (aniline, dopant, APS, and water), and different nanomaterials are produced depending upon their composition, concentration, combination of the constituents, and types of the polymerization processes employed. Therefore, one can assume that the amphiphilic dopant molecule is able to self-organize more than one form in the above process to lead to these various nanostructures.

In order to trace the mechanistic aspects of polyaniline nanomaterials formation, dynamic light scattering (DLS) analysis of the dopant (also dopant + aniline complex) in water was carried out.[38] DLS data for the dopant for concentrations $10^{-3}-10^{-5}$ M are given in Figure 5. DLS data indicate that

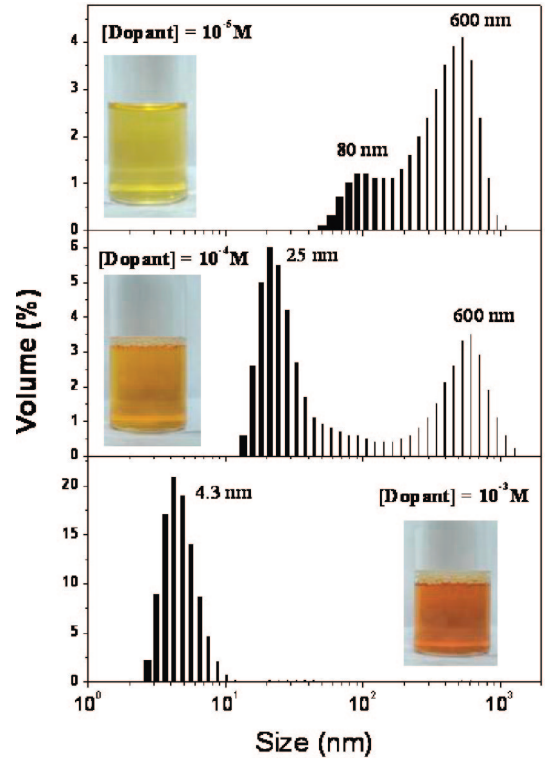

Figure 5. DLS histograms showing the size distribution of dopant aggregates in different concentrations in water at 30 °C.

more than 99.4% of the azobenzenesulfonic acid molecule exists in the form of the micelles (at 1×10^{-3} M) in water, and their average diameters were obtained as 4.29 nm. The diameter of the tightly packed spherical micelle is expected to be equal to the double length of the end-to-end distance of the molecule. It was theoretically calculated as 2×2.44 nm = 4.88 nm (see Supporting Information), which is almost matching with that of the value obtained experimentally by DLS. It confirms that the new renewable resource-based azobenzenesulfonic acid derivatives are good surfactants and form stable spherical micelles in water (more than 99%). The DLS profile of 1×10^{-4} M dopant solution shows a bimodal distribution with maxima centered at 25 and 600 nm. This indicates that as the concentration of dopant decreases in water, the strongly aggregated micelles are transformed into weakly aggregated species. Further decrease in the dopant concentration (1×10^{-5} M) increases the aggregate size to 600 nm. DLS measurement clearly demonstrates that at very lower concentrations ($1 \times 10^{-5}-5 \times 10^{-4}$ M) the dopant molecules in water are existing as open aggregates (like bilayers) and completely transformed to spherical micelles as concentration of the dopant becomes 1×10^{-3} M. The reason for the bilayer was associated with the nature of the dopant. The dopant is belonging to the push−pull type azobenzene chromophores with electron-rich hydroxyl group and electron-withdrawing sulfonic acid at both the ends, which are known to form layerlike aggregates.[39,35] Another important physical property which gives an idea about the cmc (critical micelle concentration) as well as the structural changes in anionic surfactant molecules is its specific conductance measurements.[40] For measuring the ionic conductance of the present sulfonic acid surfactant-cum-dopant, it was dissolved in deionized water to get solutions of concentration ranging from 10^{-5} to 10^{-3} M. The plot of specific conductance versus concentration of the dopant is given in Figure 6. At the dopant concentration 1×10^{-5} M the specific conductance is very low, which may be due to the number of molecules to carry the charge is very less. As the concentration of the dopant increases

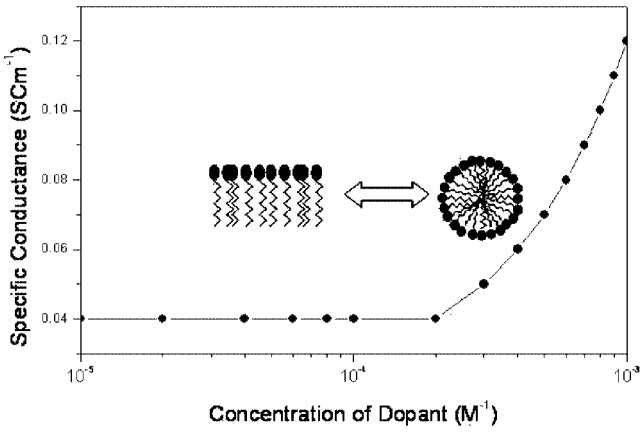

Figure 6. Plots specific conductance versus the concentration of dopant in water at 30 °C.

above 1×10^{-4} M, the specific conductance showed gradual increment marking the transformation of bilayers to small highly mobile spherical micelles, which can conduct more current. The break point of specific conductance plot directly gives the cmc[40] as $\sim 4 \times 10^{-4}$ M. The cmc of the amphiphilic azobenzene determined by specific conductance was matching with the DLS data within the margin of experimental error. The combination of DLS and conductance studies clearly evident that the dopant molecule exist in the form of bilayer assemblies below cmc and a well-defined 4.3 nm size micelles at higher concentration (above cmc).

DLS analyses of the aniline + dopant complexes at both their emulsions and dilution stages are shown in Figure 7. Upon adding aniline into the dopant micelles in water (4.3 nm), a thick emulsion was formed, and it showed a bimodal distribution with the majority of the aggregates in the range of 3−5 μm (see Figure 7 for **E-100**). DLS data for other emulsion samples (**E-150** to **E-600**) were also identical to that of **E-100** (see Supporting Information). It confirms that the aniline can form a stable aggregated emulsion with amphiphilic dopant for a wider composition (aniline/dopant = 100−600). All our attempts to get good DLS data for the polymerization mixture at aniline/dopant >900 (corresponding to the nanotubes) was not successful because of higher aniline concentration compared to that of dopant. As we diluted the reaction mixture of **E-100** by adding water, the milky appearance vanished and the resultant aniline−dopant complex showed a pale turbidity (see vials in Figure 1). DLS data showed a shift in the distribution of the aggregates size and shape from micrometer to less than 600 nm (see Figure 7 for **D-100b**). At higher dilution, the aniline + dopant complex (**D-100e**) almost become transparent and showed a narrow uniform distribution with aggregates of 175 nm. It suggests that the dilution of preaggregated microemulsion (**E-100**) leads to small nanoaggregates (**D-100e**) without any phase separation. During the interfacial polymerization, it was noticed that the addition of ammonium persulfate solution into dopant in water resulted in the formation of red turbidity. The DLS profile of the APS + dopant complex indicates that the amphiphilic dopant also has a tendency to form large 3−5 μm micrometer size aggregates with the APS. However, the nature of the distribution plot was different from that of the aniline + dopant complex. Though the DLS data give direct evidence for the existence of dopant molecule aggregates with aniline and APS and their sizes in the polymerization medium, it cannot predict the shape of the aggregates which template for nanomaterials. Therefore, it is very important to find these aggregates microscopically to trace the shape of the templates which produce fibers, tubes, rod, and spheres.[41] Interestingly, the dopant + aniline and dopant + APS complexes were stable for

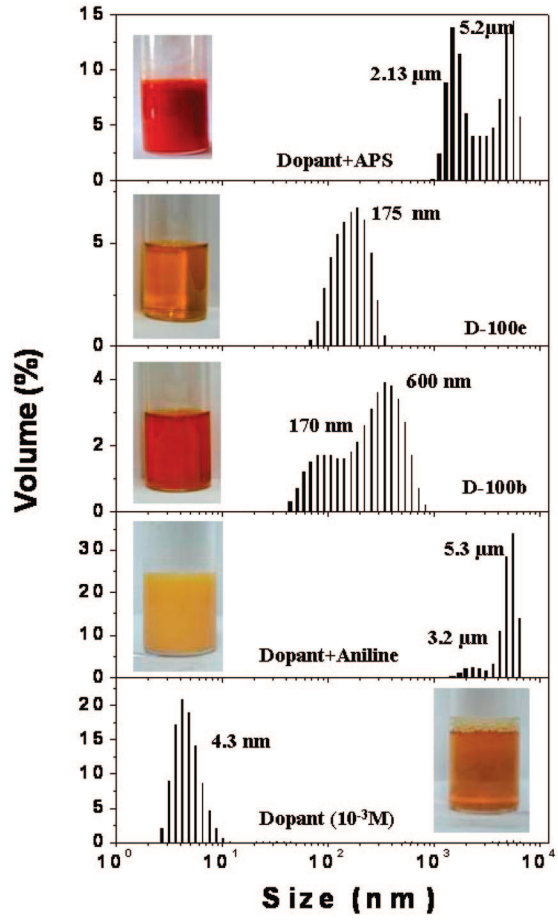

Figure 7. DLS histograms of dopant, dopant + aniline (emulsion, **E-100**), dopant + aniline (dilute), and dopant + APS (interfacial) complexes in water at 30 °C.

more than 24 h in water, which gives us the opportunity to characterize them by TEM. A drop of the emulsion, dilution template (dopant + aniline + water), and interfacial template (dopant + APS + water) were drop-cast on a TEM copper grid, which was kept on filter paper. After the initial drying of the TEM grid at the ambient conditions for 5−6 h, the trace amount of water was removed while storing the grid in a desiccator containing anhydrous calcium chloride for 1 week. High-resolution TEM images of the templates were recorded and are shown in Figure 8. The emulsion template (**E-100**) showed the presence of two types of long cylindrical micelles: (a) a longer one with diameter around 75 nm with a length of 6 μm and (b) a shorter one with 160 nm average diameter. The formation of such a long cylindrical micelles can explained in two steps: (i) the addition of aniline into spherical dopant micelles (4.3 nm evident, from DLS, Figure 5a) induced self-organization to form a thin and long cylindrical one, and (ii) these long micelles further aggregate together to form thick aggregates of diameter ranging from 80 to 180 nm. This micellar cylidrical aggregates upon oxidative polymerization by APS yields long nanofibers. The size of the micelle aggregates and the synthesized nanofibers dimensions (SEM and TEM images) are matching well with in experimental variation. This directly gives evidence for the cylindrical template mediated process in the emulsion polymerization route. The TEM images of dilute templates (**D-100e**) shows that it contains both spherical aggregates of 200 nm size plus small number of rod type aggregates (up to micrometer size). It suggests that upon dilution the long cylindrical aggregates are truncated into smaller spherical or rodlike aggregates. These spheres + rods have template for polyaniline nanorods formation in the dilute route. Interestingly, the TEM

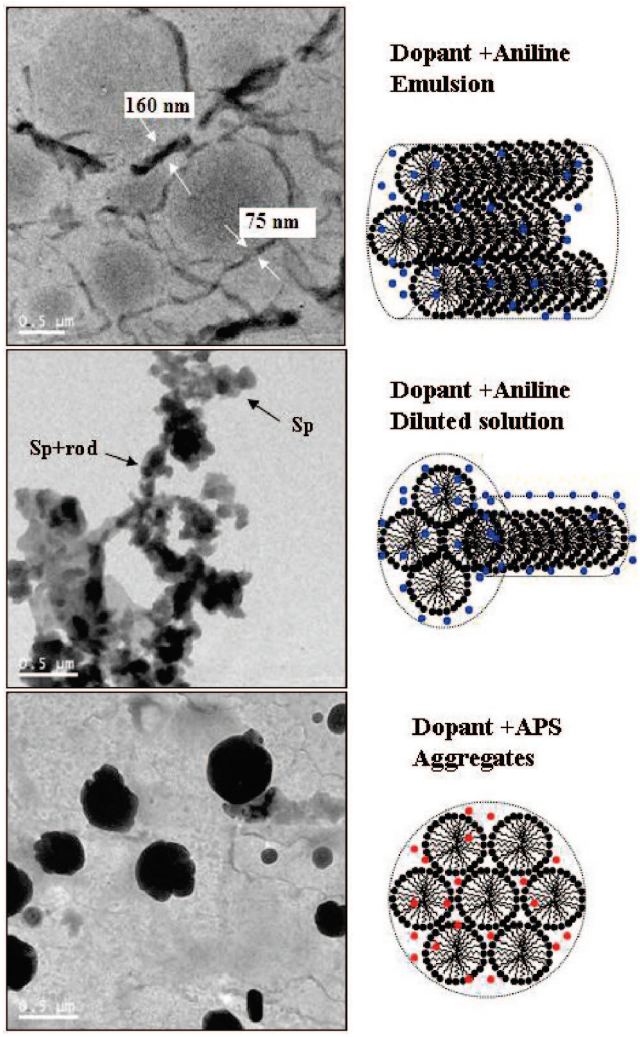

Figure 8. TEM images of the polymerization template formed by dopant + aniline and dopant + APS and their corresponding schematic representation.

image of dopant +APS complex (interfacial template) showed a completely different trend, and the templates appeared as exclusively spheres of 0.5 μm to 200 nm. In general, the interfacial route is known to produce thin nanofibers (for dopants like CSA, HCl, etc.), and for the first time, we have observed the amphiphilic dopant was producing nanospheres rather than nanofibers. In our earlier work, we have postulated that the possibility of spherical aggregates template for the synthesis of nanospheres via interfacial route.[36] Here, we proved using TEM analysis that dopant + APS complex has an unusual spherical templating behavior in the interfacial route, which produces exclusively nanospheres. It is very important to note that template identification and matching with that of the synthesized nanomaterials are very rarely reported in the literature.[42] Here, all the templates formed by the amphiphilic dopant are very stable and successfully characterized by high-resolution TEM analysis.

On the basis of the SEM and TEM morphology of the synthesized samples and template characterization by TEM and DLS, the formation of various types of nanomaterials from amphiphilic dopant is proposed in Figure 9. The dopant molecules exist in the form of 4.3 nm micelles or layerlike assemblies depending upon its concentration in water. The addition of aniline produces long micrometer range cylindrical aggregates for [aniline]/[dopant] < 600, which template for polyaniline nanofibers. At lower dopant concentration ([aniline]/[dopant] > 600), the aniline molecule trapped in the layer assemblies of dopant, which template for the polyaniline nanotubes. Because of the phase separation of aniline/dopant complex, the template for the nanotubes was not able to be characterized by DLS and TEM. Since anionic surfactants are well-known to form layer assemblies below cmc in water[43] (evident by specific conductance and DLS measurements), even in the absence of inability to view the bilayers, the proposed template model is anticipated to template for polyaniline nanotubes. The dilution of emulsion template (for fixed aniline/dopant = 100) produces micron range spheres plus rods, which aggregated together to template for polyaniline nanorods. It suggests that the effect of composition (aniline/dopant ratio) in the dopant + aniline varies the morphology from fibers to tubes, whereas the concentration gradient transforms from fibers to nanorods. In the interfacial route, the dopant forms spherical aggregates with APS. During the course of polymerization aniline monomers will diffuse from organic layer and adsorb over the spherical template surface. The subsequent oxidation of these aggregates will lead to formation of nanospheres. This is for the first time conducting polyaniline nanomaterials with a variety of nanostructures are produced from same reaction constituents through selective polymerization in water at ambient conditions. The renewable amphiphilic dopant is very unique, and it can form stable and aggregated micelles of cylindrical and layered shape for a wider range of concentrations and compositions in reaction medium to tune polyaniline nanomaterials in a single system, which is very rarely reported in the literature.

The presence of a hydrophobic tail in the dopant increases the solubility of both polyaniline nanomaterials in common organic solvents and as well as in water. Absorption spectra (see Figure 10) of polyaniline nanomaterials showed three peaks at 360, 450, and 800 nm, which are assigned as the transitions from $\pi-\pi^*$ band, polaron band to π^* band, and π band to polaron band, respectively.[44] The disappearance of the peak at 360 nm and the tail characteristics in the near-IR region above 850 nm confirmed the delocalization of the polaron band with respect to the expanded chain conformation in the polyaniline nanospheres (prepared via interfacial route).[45,46] The polyaniline nanofibers and nanorods produced via emulsion and dilution routes, respectively, showed a peak characteristic at 800 nm corresponding to coiled-like conformation.[45] The conformational changes in the polyaniline nanomaterials actually arise from their difference in the mode of chemical reactions in the polymerization processes. The interfacial polymerization is driven by the selective solubility of the polymer chains in the aqueous medium and creates more active sites at the interface for further chain growth. The higher water affinity of the charged chains has more tendencies for expanded conformation in the aqueous layer, which acts as a nucleating site for subsequent growth of expanded polyaniline nanospheres at the interface.[47] On the other hand, in the emulsion route (or dilution) such a solvent-driven unidirectional growth is not possible, and therefore, the nanofibers were obtained in entangled coiled-like conformation compared to that of the interfacial route. The presence of a hydrophobic tail in the amphiphilic dopant increases the solubility of both polyaniline nanofibers and rods in common organic solvents. The materials can be easily suspended in chloroform, *n*-butanol, *o*-chlorobenzene, *p*-xylene, and *m*-cresol, etc., which is rarely reported for polyaniline nanomaterials. It is clear from the spectra that optical density of the near-IR transitions are affected by the organic solvents; however, the conformations of the polymer nanomaterials are retained and less influenced by the solvent in which they were suspended. The absorption of polaron peaks at the lower wavelength region (~400 nm) was blue-shifted for samples recorded in organic

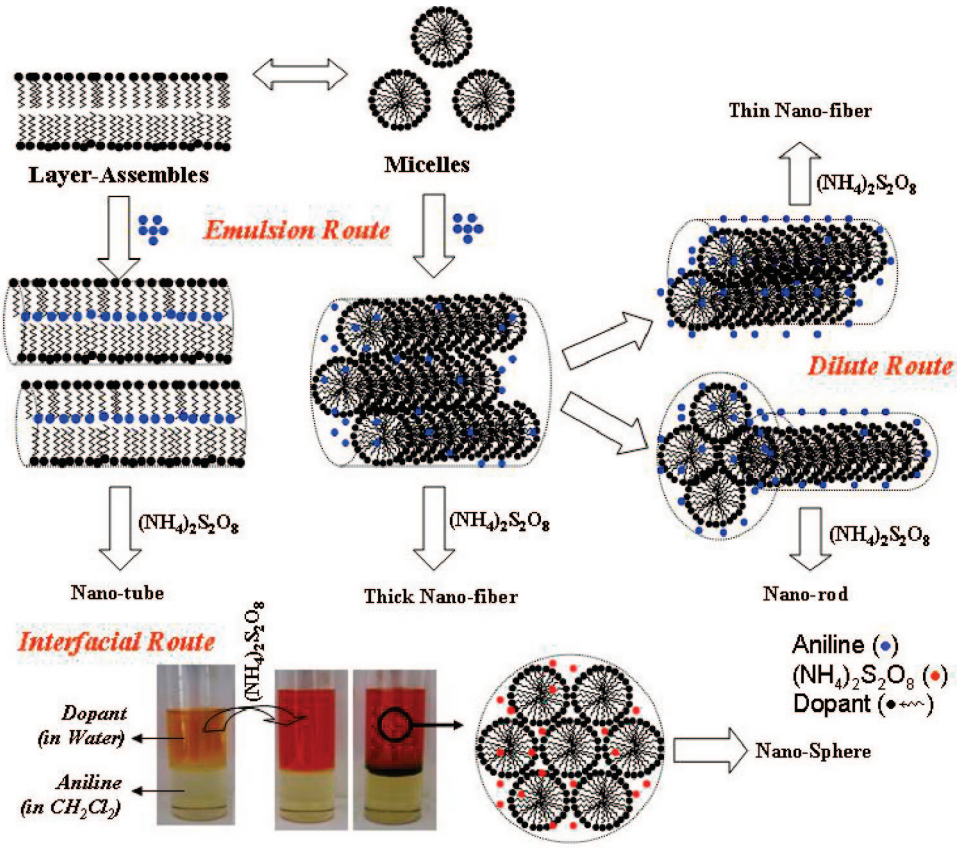

Figure 9. Plausible mechanism for the formation of polyaniline nanomaterials based on a single dopant approach via emulsion, dilute, and interfacial routes.

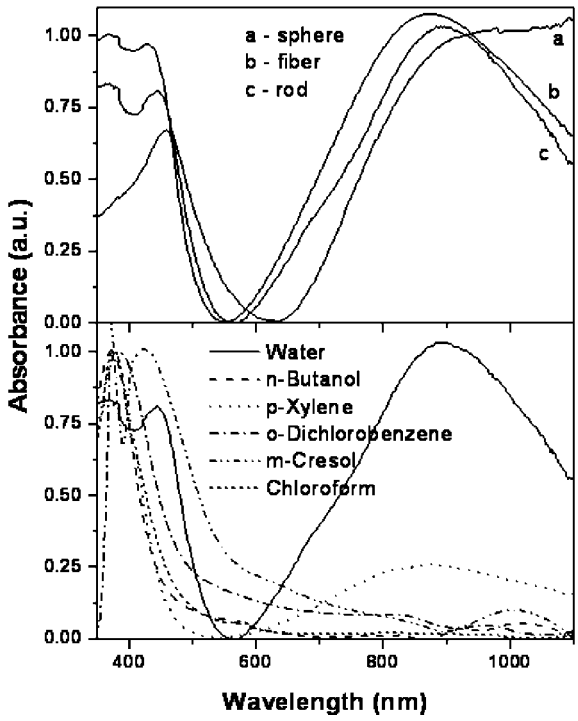

Figure 10. UV−vis spectra of all polyaniline nanomaterials (**E-100**, **I-100**, and **D-100d**) in water (top) and nanorod **D-100e** in various organic solvents (bottom) at 30 °C.

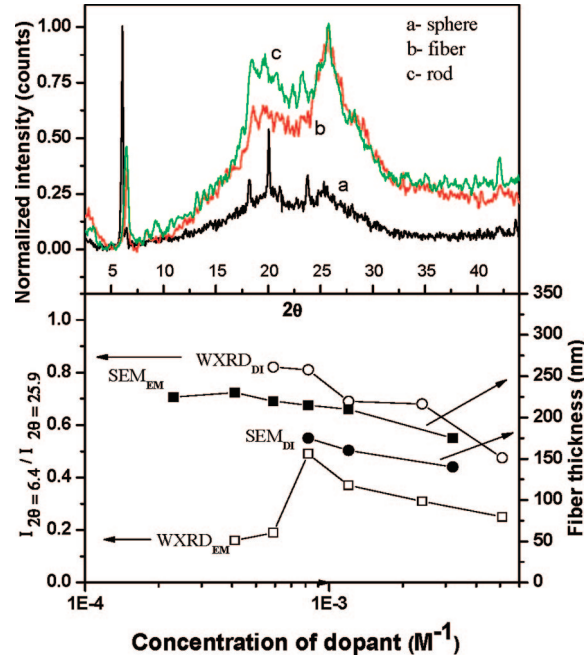

Figure 11. WXRD plots of polyaniline nanomaterials (**E-100**, **I-100**, and **D-100d**) at 30 °C (top). Plots of $I_{2\theta=6.4}/I_{2\theta=25.4}$ and fiber thickness versus the amount of dopant in the feed (bottom). The symbol DI indicates dilute route samples and EM for emulsion route samples.

solvents (except *m*-cresol) compared to that of water. The optical density of the absorption band corresponding to the polaron band of polyaniline fibers and rods (above 750 nm) were more susceptible in organic solvents, but the chain conformation is more or less retained.

The expanded chain conformation in the chains is expected to increase the solid-state ordering (or crystalline) of the nanomaterials.[44] WXRD patterns of **I-100**, **E-100**, and **D-100d**

are given in Figure 11a. All the three samples are semicrystalline with characteristic peaks at ~6.4° (d = 13.6 Å), ~20.4° (d = 4.7 Å), and ~25.3° (d = 3.5 Å).[48−50] In the case of nanofibers and nanorods the lower angle peak (~6.4°) is very sharp, and the higher angle peaks (~20° and ~25°) mostly superimposed with amorphous background scattering. The nanospheres showed a high intense sharp peak at ~6.1° (d = 14.6 Å) and also well-resolved crystalline peaks at the higher angle region, which confirmed that the nanospheres possesses (due to expanded conformation) more ordered structures compared to that of nanofibers and rods (due to coil-like conformation). Lunzy et al. studied various kinds of polyaniline materials and showed that the ratio of the intensities of the peaks at $2\theta = 6.4°$ and 26° is directly related to crystallinity of polyaniline samples.[48] The ratio of the intensities of the peaks at $2\theta = 6.4°$ and 25.9° of both emulsion and dilute route polyaniline nanomaterials and fiber thickness (from SEM images) are plotted against the concentration of dopant present in the reaction feed and are shown in Figure 11 (bottom) (for a detailed WXRD pattern, please see the Supporting Information). In the case of emulsion route sample the peak intensity ratio initially increases with decreasing dopant concentration and reaches a maximum value for sample **E-450** (around the cmc of the dopant) and then gradually decreases for low concentration of dopant. But in the case of dilution route, the peak intensity ratio increases as the volume of added water increases and finally attained the maxima at nanorods. Similarly, the average fiber thickness of the emulsion route samples is in the range 150−200 nm, whereas the thickness of the dilute route nanofibers is lower than 150 nm. This clearly indicates that upon dilution the aggregated templates break into smaller templates which led to the formation of thinner fibers. From XRD studies it is clear that in the case of nanorods the polymer chains are more ordered compared with nanofibers. The reason for the enhanced ordering in the dilute route may be correlated to the effective penetration ability of the dopant in to the polymer matrix because of the availability of isolated polymer chains. Therefore, besides the amount of dopant in the reaction mixture, the types of the polymerization routes also play a major role in controlling the solid-state properties of nanomaterials. The WXRD investigations of various polyaniline nanomaterials clearly demonstrate that the polymerization routes have a significant effect on the crystallinity of polyaniline nanomaterials.

Conclusion

We have successfully utilized the self-organization properties of new renewable resource-based amphiphilic azobenzenesulfonic acid dopant to template various polyaniline nanomaterials like nanofibers, nanotubes, nanospheres, and nanorods. The amphiphilic molecule is an efficient structure directing dopant for polyaniline nanomaterials and has template selectivity depending upon the dopant/aniline ratio as well as concentration of dopant and aniline. DLS and TEM techniques have been successfully utilized to trace the nature and shape of polymerization templates to understand the mechanism the nanomaterials formation. The present investigation brought the following outcomes: (i) the dopant molecules exist as spherical micelles of 4.3 nm above the cmc (6×10^{-4} M) and bilayers at concentrations lower than the cmc, (ii) the micelle characteristics of the dopant were done by DLS and specific conductance measurements, (iii) the dopant micelles have shape selective self-organization with aniline and APS, (iv) at concentration higher than cmc of the dopant, well-defined micrometer-sized cylindrical micelles filled with aniline act as templates for the growth of long nanofibers, (v) as the concentration of the dopant below cmc, the bilayers filled with aniline are acting as templates for the growth of nanotubes, (vi) in the dilute polymerization, the size of the aggregates becomes 175 nm and consists of spherical plus short cylindrical micelle aggregates, which upon chemical oxidation yields nanorods, (vii) in the interfacial route, the dopant micelles form spherical aggregates with APS in the aqueous layer and the diffusion of aniline (through interfacial layer) into these spherical aggregates and get oxidized to form polyaniline spheres of 200−400 nm, (viii) the structures of the cylindrical and spherical micelle templates were characterized by DLS and high-resolution TEM, (ix) absorption spectra of the nanomaterials revealed that the nanospheres possesses expanded confirmation and the fibers, rods, and tubes were found to have coil-like confirmation, and (x) wide-angle X-ray diffraction showed that the nanomaterials exhibit good solid-state ordering compared with conventional polyaniline because of the high penetrating power of amphiphilic dopant in to polymer matrix. In a nutshell, we have shown for the first time that divergent polyaniline nanomaterials such as fibers, rods, tubes, and spheres can be synthesized from identical reactant ingredients by carefully choosing the amphiphilic dopant templates under emulsion, dilution, and interfacial polymerizations.

Acknowledgment. We thank the Department of Science and Technology, New Delhi, India, under Scheme NSTI Programme-SR/S5/NM-06/2007 for financial support. The authors thank Dr. Peter Koshy, Mr. M. R. Chandran, Dr. V. S. Prasad, Dr. U. Syamaprasad and Mr. P. Gurusamy, NIIST-Trivandrum, for SEM, TEM, and WXRD analyses. We also thank Mr. Willi Paul, SCTIMST, Trivandrum, for dynamic light scattering analysis. P. Anilkumar thanks UGC-New Delhi, India, for a senior research fellowship.

Supporting Information Available: Additional information for synthesis and characterization of the dopant, table containing the amount of water added for dilute polymerization, FT-IR spectra of the nanomaterials, TEM image of Y-junction nanotubes, SEM images of polyaniline nanofibers synthesized under different experimental conditions, theoretical AM1 model of dopant molecule, DLS details, and size plots of emulsions (**E-100**, **E-600**, **E-900**), WXRD plots of polyanilines, and TGA plots of nanomaterials. This material is available free of charge via the Internet at http://pubs.acs.org.

References and Notes

(1) Lee, K.; Cho, S.; Park, S. H.; Heeger, A. J.; Lee, C. W.; Lee, S. H. *Nature (London)* **2006**, *441*, 65–68.
(2) MacDiarmid, A. G. *Angew. Chem., Int. Ed.* **2001**, *40*, 2581–2590.
(3) Alam, M. M.; Wang, J.; Guo, Y.; Lee, S. P.; Tseng, H. R. *J. Phys. Chem. B* **2005**, *109*, 12777–12784.
(4) Haung, J.; Virji, S.; Kaner, R. B.; Weiller, B. H. *Nano Lett.* **2004**, *4*, 491–496.
(5) Qiao, Y.; Bao, S. J.; Li, C. M.; Cui, X. Q.; Lu, Z. S.; Guo, J. *ACS Nano* **2008**, *1*, 113–119.
(6) Haung, J.; Virji, S.; Weiller, B. H.; Kaner, R. B. *Chem.—Eur. J.* **2004**, *10*, 1314.
(7) Janata, J.; Josowicz, M. *Nat. Mater.* **2002**, *2*, 19–24.
(8) Hatchett, D. W.; Josowicz, M. *Chem. Rev.* **2008**, *108*, 746–769.
(9) Zhang, Z.; Wei, Z.; Wan, M. X. *Macromolecules* **2002**, *35*, 5937–5942.
(10) Liu, J.; Lin, Y.; Liang, L.; Voigt, J. A.; L. Huber, D.; Tian, Z. R.; Coker, E.; Mckenzie, B.; Mcdermott, M. J. *Chem.—Eur. J.* **2003**, *9*, 604.
(11) Martin, C. R. *Acc. Chem. Res.* **1995**, *28*, 61.
(12) Carswell, A. D. W.; O'Rear, E. A. O.; Grady, B. P. *J. Am. Chem. Soc.* **2003**, *125*, 14793–14800.
(13) Cai, Z.; Martin, C. R. *J. Am. Chem. Soc.* **1989**, *111*, 4138.
(14) Wei, Z.; Zhang, Z.; Wan, M. X. *Langmuir* **2002**, *18*, 917–921.
(15) Han, J.; Song, G.; Guo, R. *Adv. Mater.* **2007**, *19*, 2993.
(16) Yan, Y.; Yu, Z.; Huang, Y. W.; Yuan, W. X.; Wei, Z. X. *Adv. Mater.* **2007**, *19*, 3353.
(17) Li, G.; Zhang, Z. *Macromolecules* **2004**, *37*, 2683–2685.
(18) Meng, L.; Lu, Y.; Wang, X.; Zhang, J.; Duan, Y.; Li, C. *Macromolecules* **2007**, *40*, 2981–2983.

(19) Li, C.; Hatano, T.; Takeuchi, M.; Shinkai, S. *Chem. Commun.* **2004**, 2350–2351.
(20) Zhang, Z.; Wei, Z.; Wan, M. X. *Macromolecules* **2002**, *35*, 5937–5942.
(21) Haung, J.; Virji, S.; Weiller, B. H.; Kaner, R. B. *J. Am.Chem. Soc.* **2003**, *125*, 314.
(22) Haung, J.; Kaner, R. B. *J. Am. Chem.Soc.* **2004**, *126*, 851–855.
(23) Haung, J.; Kaner, R. B. *Angew. Chem.* **2004**, *116*, 5941–5945.
(24) Zhang, X.; Goux, W. J.; Manohar, S. K. *J. Am. Chem. Soc.* **2004**, *126*, 4502–4503.
(25) Chiou, N. R.; Epstein, A. J. *Adv. Mater.* **2005**, *17*, 1679–1683.
(26) Chiou, N. R.; Epstein, A. J. *Synth. Met.* **2005**, *153*, 69–72.
(27) Zhou, C.; Han, J.; Guo, R. *J. Phys. Chem. B* **2008**, *112*, 5014–5019.
(28) Li, D.; Kaner, R. B. *J. Am. Chem. Soc.* **2006**, *128*, 968–975.
(29) Jing, X.; Wang, Y.; Wu, D.; She, L.; Guo, Y. *J. Polym. Sci., Part A: Polym. Chem.* **2006**, *44*, 1014–1019.
(30) Haung, K.; Wan, M. X. *Chem. Mater.* **2002**, *14*, 3486–3492.
(31) Chiou, N. R.; Lu, C.; Guan, J.; Lee, L. J.; Epstein, A. J. *Nat. Nanotechnol.* **2007**, *2*, 354–357.
(32) Chiou, N. R.; Lee, L. J.; Epstein, A. J. *Chem. Mater.* **2007**, *19*, 3589–3591.
(33) Anilkumar, P.; Jayakannan, M. *Langmuir* **2006**, *22*, 5952–5957.
(34) Jinish Antony, M.; Jayakannan, M. *J. Phys. Chem. B* **2007**, *111*, 12772–12780.
(35) Anilkumar, P.; Jayakannan, M. *J. Phys. Chem. C* **2007**, *111*, 3591–3600.
(36) Anilkumar, P.; Jayakannan, M. *Macromolecules* **2007**, *40*, 7311–7319.
(37) Xia, H.; Narayanan, J.; Cheng, D.; Xiao, C.; Liu, X.; Chan, H. S. O. *J. Phys. Chem. B* **2005**, *109*, 12677–12684.
(38) (a) Zhang, X.; Kolla, H. S.; Wang, X.; Raja, K.; Manohar, S. K. *Adv. Funct. Mater.* **2006**, *16*, 1145–1152. (b) Hassan, P. A.; Sawant, S. N.; Bagkar, N. C.; Yakhmi, J. V. *Langmuir* **2004**, *20*, 4874–4880.
(39) Shimomura, M.; Kunitake, T. *J. Am. Chem. Soc.* **1987**, *109*, 5175–5183.
(40) Atkins, P.; de Paula, J. *Atkin's Physical Chemistry*, 7th ed.; Oxford University Press: New York, 2002; Chapter 21, p 755.
(41) Zhang, L.; Wan, M. X. *Adv. Funct. Mater.* **2003**, *13*, 815–820.
(42) Wei, Y.; Zhang, L.; Yu, M.; Yang, Y.; Wan, M. X. *Adv. Mater.* **2003**, *15*, 1382–1385.
(43) Johnsson, M.; Wagenaar, A.; Engberts, J. B. F. N. *J. Am. Chem. Soc.* **2003**, *125*, 757–760.
(44) Xis, Y.; Wiesinger, J. M.; MacDiarmid, A. G. *Chem. Mater.* **1995**, *7*, 443–445.
(45) MacDiarmid, A. G.; Epstein, A. J. *Synth. Met.* **1995**, *69*, 85–92.
(46) Min, Y.; Xia, Y.; MacDiarmid, A. G.; Epstein, A. J. *Synth. Met.* **1995**, *69*, 159–160.
(47) Li, W.; Zhu, M.; Zhang, Q.; Chen, D. *Appl. Phys. Lett.* **2006**, *89*, 103110.
(48) Lunzy, W.; Banka, E. *Macromolecule.* **2000**, *33*, 425.
(49) Jana, T.; Nandi, A. K. *Langmuir* **2000**, *16*, 3141.
(50) Jayakannan, M.; Annu, S.; Ramalekshmi, S. *J. Polym. Sci., Polym. Phys.* **2005**, *43*, 1321.

MA801090F